

# Carboxylic acid adsorption on NiO(100) characterized by X-ray photoelectron and high resolution electron energy loss spectroscopies

K.W. Wulser and M.A. Langell \*

*Department of Chemistry, University of Nebraska, Lincoln, NE 68588-0304, USA*

Formic, acetic and propionic acids have been adsorbed onto NiO(100) at 300 K and the resulting species characterized by X-ray photoelectron spectroscopy (XPS) and high resolution electron energy loss spectroscopy (HREELS). As do many ionic solids, nickel oxide possesses a strong series of Fuchs–Kliwer multiple phonon losses, which obscures the weaker adsorbate vibrational structure. A novel phonon deconvolution procedure that removes multiple phonons has, therefore, been used in analyzing the HREELS data. NiO(100) exhibits amphoteric chemisorptive properties, dissociatively adsorbing the acids as carboxylates and surface hydroxyls. Adsorption saturates after approximately 10000 langmuir to yield one carboxylate for every two nickel sites. By stoichiometry, one half of all surface oxygen sites are assumed to be hydroxylated. A tilted carboxylate geometry is evident in the high value of the  $\nu_s(\text{COO})$  vibrational mode observed in the HREEL spectra.

**Keywords:** HREELS; XPS; NiO(100); formic acid; acetic acid; propionic acid

## 1. Introduction

There is much evidence that the stability of carboxylate intermediates is important in determining product selectivity in the catalytic synthesis of methanol and other oxygenates from CO and H<sub>2</sub> [1–3]. In particular, it has been shown that carboxylates are stabilized at metal surfaces when the substrate is predosed with oxygen [3–8], the oxygen serving to increase the Brønsted basicity of the adsorption sites. Studies of transition metal oxides and thin oxide films [9–14] show that these surfaces also have a tendency to form stable carboxylates through the acid–base mechanisms. However, metal oxide studies are significantly fewer in number than those performed for their transition metal analogs.

We present evidence for the formation of carboxylates at NiO(100) upon exposure of the single crystal to formic, acetic and propionic acids at  $3 \times 10^{-4}$

Pa and 300 K. Nickel oxide is an ideal model substrate for adsorption studies since large single crystal samples with reliable structural and compositional integrity can readily be procured. The rocksalt structure yields a very stable (100) nonpolar surface where cationic and anionic Coulombic interactions are efficiently balanced [15]. Thus, the surface has been found to terminate in the simple, unreconstructed form of the bulk lattice [16–18] and provides well-defined adsorption sites.

Since surface-sensitive techniques were developed primarily in the study of pure metals, the metal oxides are considered relatively “inert” in their adsorption properties and considerable effort has been made to activate them to adsorb gases more rapidly or in greater amount. For NiO(100), activation has generally taken the form of  $\text{Ar}^+$  bombardment- [15,19,20] or  $\text{H}_2$  reduction- [19,20] induced vacancy formation and the gases studied are often those that might be expected to replace lattice oxide vacancies ( $\text{O}_2$ ,  $\text{H}_2\text{O}$ , methanol [21,22]). Even heavily defect-laden NiO(100) surfaces, however, have typically required exposures of megalangmuirs [21] or even teralangmuirs [22] for detectable quantities of adsorbate to form by this mechanism.

Carboxylic acid adsorption makes use of the amphoteric nature of the NiO(100) surface to adsorb the acid dissociatively as carboxylate and surface hydroxyl. The NiO(100) used in this study is stoichiometric to within the limits of detection and no deliberate attempts to induce defect formation have been made. For all three acids, the surface saturates to carboxylate formation after  $\approx 10000$  langmuir (L). While perhaps appearing long in comparison to pure transition metal substrates, these exposures are considerably shorter than the majority of successful adsorbate studies reported for single crystal NiO(100) to date.

In the sections below, X-ray photoelectron spectroscopy (XPS) will first be used to identify the carboxylates and to estimate saturation coverages. Once unequivocally identified by XPS [7,13,14,23], the carboxylates are then studied by high resolution electron energy loss spectroscopy (HREELS). The HREEL spectra confirm the presence of the carboxylate and give additional information about the bonding configuration.

As expected for a high quality NiO(100) surface [22,24,25], the HREEL spectrum shows a well developed Fuchs–Kliwer phonon multiple loss progression due to collective vibrations of the metal oxide lattice [26]. Because of strong dipolar coupling between the phonons and the electron beam, the adsorbate vibrational spectrum is almost totally obscured by the substrate phonon structure. Since all information on the multiple losses is contained in the single loss phonon peak [26,27], the multiple losses have been deconvoluted from the desired single loss spectrum in the data below. While the deconvolution algorithm is outlined in the text, space limitation precludes an in depth discussion of the deconvolution procedure. Several recent publications describe the algorithm and its application in detail [22,27].

## 2. Experimental

The ultrahigh vacuum (UHV) chamber used in these studies has been previously described in detail [20]. Most relevant to these studies are the Physical Electronics ( $\Phi$ ) 15-225C double pass cylindrical mirror analyzer (CMA) and 04-548 dual Al/Mg anode used in XPS, the  $\Phi$  15-120 low energy electron diffraction (LEED) optics and the in-house built single pass 127° sector HREEL spectrometer \*. The CMA is also equipped with a 5 keV coaxial electron gun for Auger analysis.

A NiO single crystal of  $\approx 5 \times 5 \times 1 \text{ mm}^3$  \*\* and oriented to within 1° of the (100) face was polished with successively finer grades of alumina to 0.03  $\mu\text{m}$  final abrasive grit. The sample was mounted with thin tantalum straps to a titanium backing plate machined to fit the crystal dimensions and a chromel–alumel thermocouple was spot welded to the edge of the plate to provide an estimate of temperature for cleaning purposes. The backing plate was then suspended between two tantalum wires for attachment to the goniometer. The wires also provided resistive heating to  $\approx 1000 \text{ K}$ .

The integrity of the NiO(100) surface was determined with Auger, XPS, HREELS and LEED. When first placed in UHV, the sample was invariably covered with multilayers of a mixed phase oxide. The surface was cleaned by repeated cycles of argon ion bombardment (2 kV, 4  $\mu\text{A}$ ,  $4 \times 10^{-3} \text{ Pa}$  argon) at 300 K, followed by annealing at 800 K under  $5 \times 10^{-5} \text{ Pa O}_2$ . A final oxygen anneal cycle was followed by 10 min anneal at 800 K in UHV. Important to ensuring NiO(100) surface integrity are well defined LEED of proper symmetry and lattice spacing, XPS binding energies and satellite structure appropriate to stoichiometric NiO and a high quality HREELS phonon progression at integral multiples of the 70.5 meV ( $564 \text{ cm}^{-1}$ ) single loss phonon. All XPS binding energies have been referenced to the O 1s peak previously calibrated to be 529.4 eV [20]. The  $\text{Ni}^{2+} 2p_{3/2}$ ,  $2p_{1/2}$  binding energies are 853.3 and 871.7 eV, respectively.

The HREEL spectra were taken in the specular mode at 60° relative to the surface normal with an electron beam energy of 2.7 eV. While the spectrometer has an ultimate resolution of  $\approx 7\text{--}8 \text{ meV}$  ( $56\text{--}64 \text{ cm}^{-1}$ ) with conducting substrates, it was somewhat less ( $80\text{--}120 \text{ cm}^{-1}$  FWHM for  $1 \times 10^5 \text{ cps}$ ) for the more poorly conducting NiO(100) crystal. This resolution is comparable to or better than that currently reported in the literature for NiO [24,25].

The formic, acetic and propionic acids were purified by refluxing with chromate, followed by redistillation and multiple freeze–thaw cycles to drive off dissolved gases [28]. Exposures of 10000 L were used for each gas at pressures of

\* Designed by J. Gland, University of Michigan, with blueprints adapted by J.M. White, University of Texas-Austin.

\*\* Kindly supplied by N. Peterson, Materials Science Division, Argonne National Laboratory.

$3 \times 10^{-4}$  Pa uncorrected Bayard–Alpert gauge. All exposures and subsequent measurements were performed at 300 K.

### 3. Data

When NiO(100) is exposed to 10000 L of formic, acetic and propionic acids, the XP spectra of figs. 1 and 2 result. The O 1s spectral ranges for formate, acetate and propionate are shown in figs. 1a, 1b and 1c, respectively. In each case, the dominant peak to lower binding energy results from lattice oxygen at

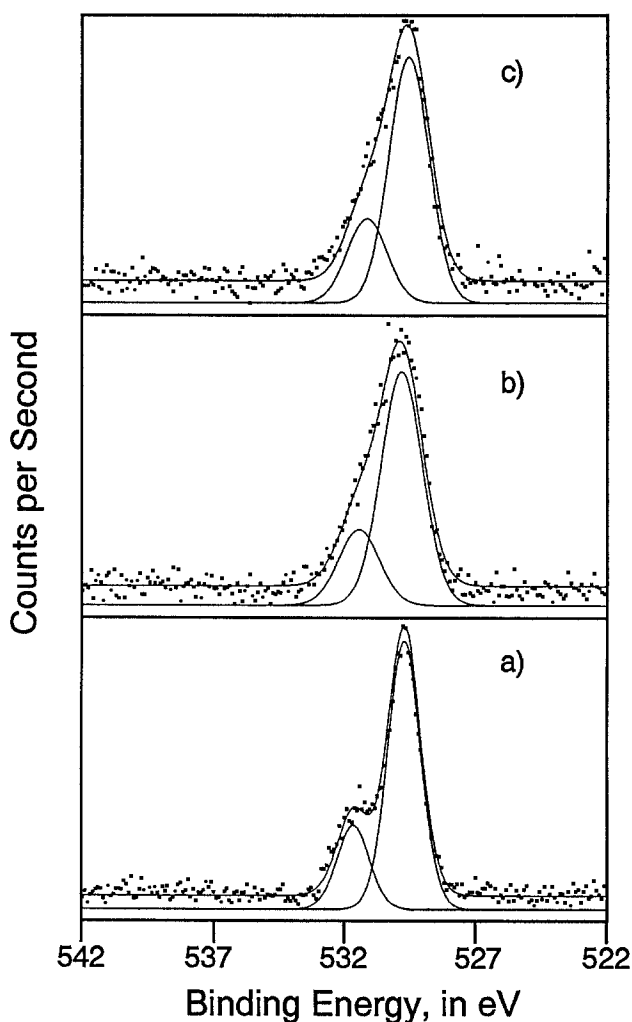


Fig. 1. O 1s XP spectra of (a) formate, (b) acetate and (c) propionate. The spectra were acquired using Mg  $K_{\alpha}$  radiation at 25 eV pass energy.

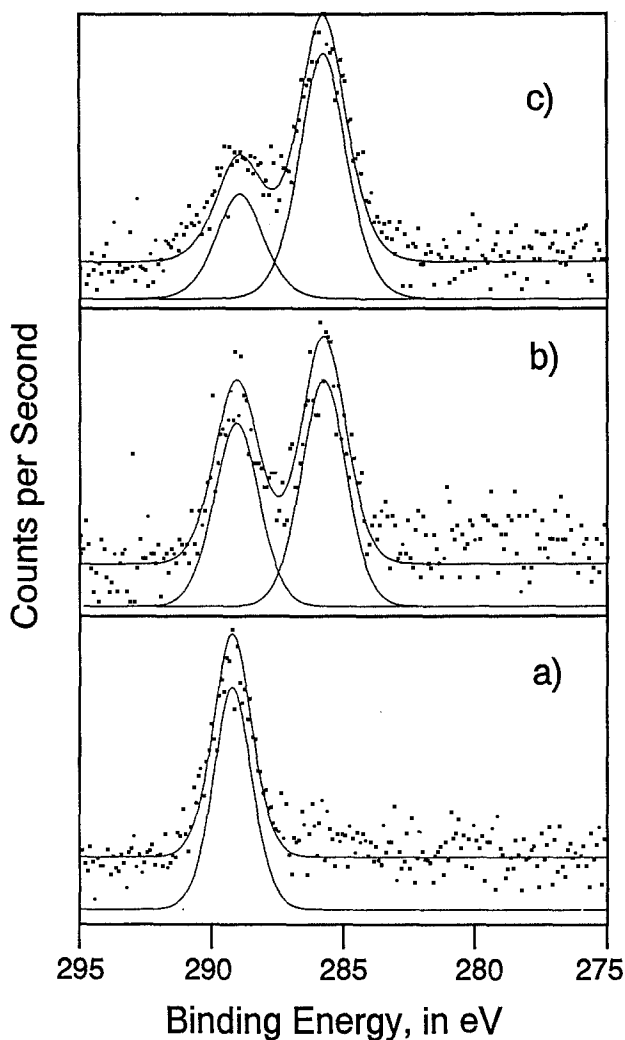


Fig. 2. C 1s XP spectra of (a) formate, (b) acetate and (c) propionate on NiO(100). The spectra were acquired using Mg  $K_{\alpha}$  radiation at 50 eV pass energy.

529.4 eV. The shoulder to higher binding energy was resolved with curve-fitting techniques [29,30] and the discrete points in the figure are the actual data with the solid lines the result of the curve fit. The peak shapes are primarily Gaussian, with a 30% Lorentzian admixture.

Adsorbate O 1s binding energies are found to be  $531.2 \pm 0.2$  eV, in agreement with literature values for adsorbed carboxylates [7,13,14,23], and are summarized in table 1. Note the absence of any significant O 1s intensity for binding energies of 533 eV or greater, as would be expected if significant amounts of the parent acids had adsorbed molecularly or if  $H_2O$  had formed

Table 1

Binding energies of XP spectras. All energies are given in eV

	Formate	Acetate	Propionate
carboxyl C C 1s	288.4	288.0	287.8
aliphatic C C 1s	—	284.7	284.6
lattice O 1s	529.4	529.4	529.4
hydroxyl and carboxylate O 1s	531.4	531.3	531.0

through condensation of surface hydroxyls and/or parent acid protons. Unfortunately, surface hydroxyls cannot be resolved from the carboxylates in the O 1s XP spectral region, although the HREELS data described below show them clearly to be present. We therefore assume the O 1s adsorbate peak to contain contributions from both carboxylate and surface hydroxyl and fit them as a single feature.

The data in fig. 1 can also be used to estimate the adsorbate coverage. Assuming an exponential attenuation of photoelectron intensity with depth into the crystal, the relative coverage of adsorbate oxygen,  $C_{\text{ads}}$ , to substrate oxygen,  $C_{\text{oxide}}$ , can be calculated from

$$\frac{I_{\text{ads}}}{I_{\text{oxide}}} = \frac{C_{\text{ads}}}{\sum_1^{\infty} C_{\text{oxide}} \exp(-nx \cos \theta / \lambda)}, \quad (1)$$

where  $I_{\text{ads}}/I_{\text{oxide}}$  is the relative adsorbate to lattice oxide O 1s intensity,  $x = 2.1$  Å is the spacing between crystal layers along  $\langle 001 \rangle$ ,  $\theta$  is the detection angle of the CMA, and  $\lambda$  is the mean free path of the O 1s photoelectron, taken as 11 Å [31] for electron kinetic energies of  $\approx 725$  eV in the Mg  $K_{\alpha}$ -generated XP spectra.

In applying eq. (1) to the carboxylate-covered NiO(100) surface, it has been assumed that the carboxylate does not attenuate the underlying lattice oxide signal and that all carboxylic acid protons react to form surface hydroxyls through their interaction with lattice oxygen. The latter reaction removes lattice oxide contributions to XPS in the outermost layer and transfers the intensity to the hydroxyl/carboxylate shoulder. Thus, one third of the adsorbate O 1s intensity at  $\approx 531.2$  eV is due to surface hydroxyl and the remaining two thirds are due to the two carboxylate oxygens. Therefore  $C_{\text{oxide}} = 0.5 - \frac{1}{3}C_{\text{ads}}$  for  $n = 0$ , the outermost surface layer, and  $C_{\text{oxide}} = 0.5$  for  $n \geq 1$ , as appropriate for a fractional oxide concentration of  $\frac{1}{2}$  in NiO.

The total coverage of adsorbate oxygen obtained from eq. (1) is  $\approx 0.75$  monolayers (ML) for each of the carboxylates adsorbed on NiO(100). The net coverage, assuming stoichiometric quantities of carboxylate and hydroxyl, is therefore  $\approx 0.25$  ML, or approximately one carboxylate species to every two

Table 2  
Relative ratios of species in XPS

	Formate	Acetate	Propionate
$O_{\text{carboxy}}/O_{\text{lattice}}$	0.24/0.76	0.25/0.75	0.24/0.76
$C_{\text{aliphatic}}/C_{\text{carboxy}}$	0/1	0.55/0.45	0.69/0.31

surface nickel sites. In addition, 50% of the surface lattice oxygen sites are assumed to be hydroxylated.

The carbon 1s XP spectra (fig. 2) are noisier than the O 1s data due to the lower cross-section for carbon photoelectrons. A single carbon peak is observed for the formate (fig. 2a) at 288.4 eV in agreement with literature values [7,13,14,23]. Note the absence of peaks at  $\approx 285$  eV, which would be observed if  $CH_x$  fragments were to form through adsorbate decomposition, and at  $\geq 290$  eV characteristic for molecularly adsorbed formic acid and surface carbonates.

The acetate and propionate C 1s spectra (figs. 2b and 2c) are each fitted to two C 1s peaks to yield values appropriate for carboxylate and aliphatic portions of the adsorbate species. Using curve fitting techniques, the relative intensity is determined to be approximately 1/1 and 2/1 for aliphatic to carboxylate carbons in the acetate and propionate, respectively. The binding energies and relative concentrations for the XPS data are summarized in tables 1 and 2.

HREEL spectra of the acetate are shown in fig. 3, with the “as obtained” spectrum given in fig. 3a and a post deconvolution spectrum in fig. 3b. Prior to deconvolution, the hydroxyl stretching mode is observed at  $\nu(\text{OH}) = 3588 \text{ cm}^{-1}$ , and the aliphatic hydrocarbon stretch is distinguishable at  $\nu = 3075 \text{ cm}^{-1}$ , although the phonon structure of the NiO lattice obscures other useful adsorbate modes. The  $3588 \text{ cm}^{-1}$  peak may contain some unresolved contribution from  $\nu(\text{CH})$  stretching plus single loss phonon combination. The spectrum also confirms the absence of molecularly adsorbed acid, which would give rise to a characteristic  $\nu(\text{COOH})$  stretch at approximately  $2700 \text{ cm}^{-1}$  [8].

The deconvolution algorithm used to obtain fig. 3b assumes that the phonon intensities decrease in a Poisson distribution for the phonon spectrum  $p(\omega)$  [26,27]:

$$s(\omega) = i(\omega) \otimes \left[ \delta(0) + p(\omega) + \frac{p(\omega) \otimes p(\omega)}{2!} + \frac{p(\omega) \otimes p(\omega) \otimes p(\omega)}{3!} + \dots \right]. \quad (2)$$

The symbol  $\otimes$  represents mathematical convolution,  $i(\omega)$  is the instrument response function and  $\delta(0)$  is the elastic peak whose peak shape is determined entirely by  $i(\omega)$ . In the present HREEL spectra,  $i(\omega)$  is chosen by fitting the

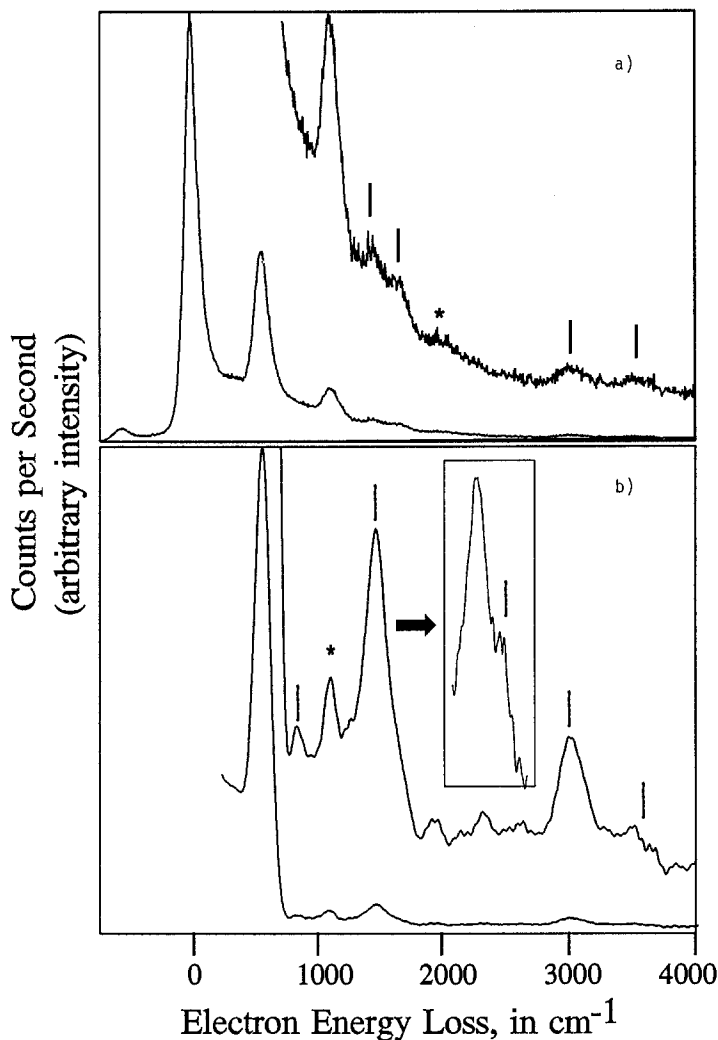


Fig. 3. HREEL spectra of the NiO(100)–OOCCH<sub>3</sub> surface (a) prior and (b) post deconvolution. Inset in (b) is of the  $\nu(\text{COO})$  range taken at higher resolution, with the dash marking the  $\nu_a(\text{COO})$  peak. Peaks marked with \* are due to incomplete removal of multiple excitation phonon intensity.

elastic peak with a Gaussian–Lorentzian function [22,30]. Upon Fourier transformation

$$S(\tau) = I(\tau) \left[ 1 + P(\tau) + \frac{P(\tau)^2}{2!} + \frac{P(\tau)^3}{3!} + \cdots \right]. \quad (3)$$

The quantity in square brackets is an expansion of  $e^{P(\tau)}$ :

$$P(\tau) = \ln[S(\tau)/I(\tau)]. \quad (4)$$



After back transformation, the single loss spectrum is in principle obtained free from contamination by higher multiples:

$$p(\omega) = \mathcal{F}^{-1}\{\ln[S(\tau)/I(\tau)]\}. \quad (5)$$

In practice, the phonon distribution is not perfectly harmonic and not all of the multiple phonon intensity is removed. The residual phonons have been greatly suppressed, however, and now are comparable to the adsorbate spectrum in intensity. Unremoved residual “harmonics” occur predictably at integral multiples of the single loss phonon peak and thus can be distinguished from adsorbate vibrational modes. The elastic peak is removed during deconvolution and data below the single phonon excitation peak is, therefore, lost. Depending upon the instrument response function  $I(\tau)$  chosen, the spectrum is also smoothed and somewhat broadened. Application of eq. (5) is described in more detail elsewhere [22,24].

After deconvolution, additional adsorbate losses are observed at 860, 1302, 1502, and 1650  $\text{cm}^{-1}$  with a small peak at 1975  $\text{cm}^{-1}$  from concentrations of CO which were too low to be detected by XPS. The peak at 1128  $\text{cm}^{-1}$  is due to an incompletely removed double phonon excitation ( $2 \times 564 \text{ cm}^{-1}$ ) as is a much weaker peak at 2256 ( $4 \times 564 \text{ cm}^{-1}$ ). Presumably, the unremoved portion of the triple loss is obscured by the now significantly more intense adsorbate peaks.

Fig. 4 shows the results of the deconvolution applied to the formate (fig. 4a) and propionate (fig. 4c), along with the acetate (fig. 4b) just described. Vibrational assignments are given in table 3 and agree well with literature values for carboxylates found on metal [8,31] and metal oxide surfaces [9]. Two additional features should be mentioned. When the resolution of the HREEL spectra is good enough, a  $\nu(\text{M}-\text{O}) + \nu_s(\text{COO})$  combination band can be fortuitously detected at  $\approx 1800 \text{ cm}^{-1}$ , allowing information to be obtained on the  $\nu(\text{M}-\text{O})$  adsorbate–substrate stretch by difference. This portion of the HREEL spectrum is otherwise lost during the deconvolution analysis.

Secondly, while the vibrational energies agree well with those reported for carboxylates in general, the  $\nu_s(\text{COO})$  features are at the high end of the observed values. High carboxylate symmetric stretch frequencies have been correlated with a tilted adsorbate structure [8,31] discussed in detail below.

#### 4. Discussion

The NiO(100) formic, acetic and propionic adsorbates show that the acid–base character of NiO can be used at the relatively high substrate temperature of 300 K to yield saturation concentrations of carboxylate plus surface hydroxyl. XPS unambiguously identifies the carboxylate species and determines saturation concentrations to be approximately one carboxylate for every two nickel sites. While small quantities of defects are undoubtably present, the high carboxylate

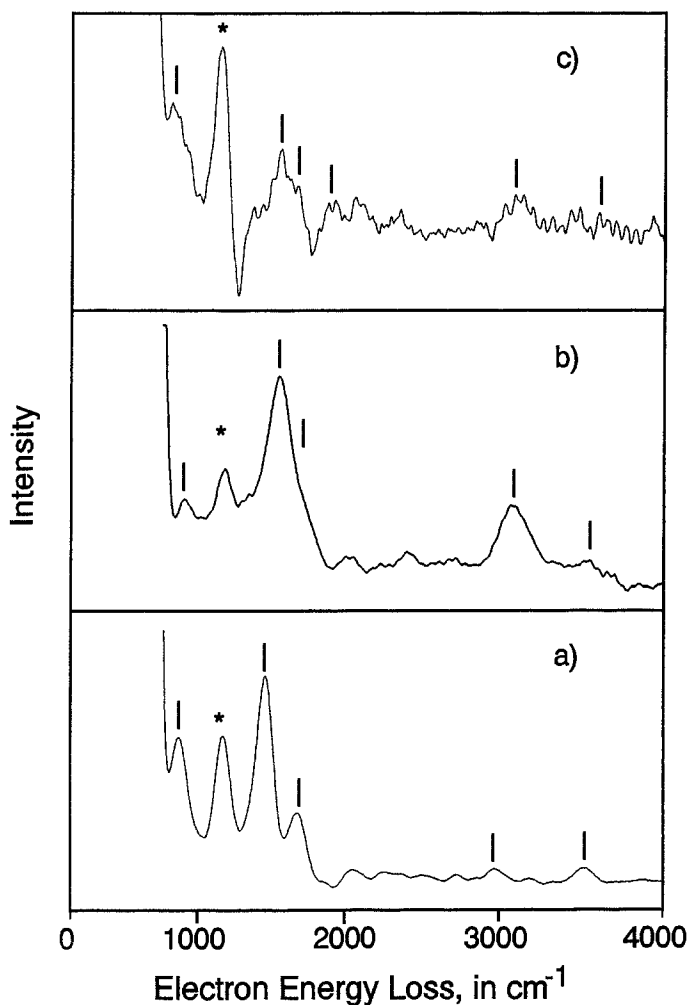


Fig. 4. HREEL postdeconvolution spectra of (a) formate, (b) acetate and (c) propionate on NiO(100). Peaks marked with \* are due to incomplete removal of the surface phonons.

concentrations indicate that defects are not directly associated with the adsorbate site. Furthermore, while 10000 L might appear to be a long exposure in comparison with metal adsorption, it is short for single crystal NiO(100) where significantly longer exposures have been required to obtain detectable amounts of adsorbates with other gases [21,22].

HREEL data confirm the assignment of the carboxylates and show the presence of surface hydroxyl. The hydroxyl could not be distinguished from carboxylate in the O 1s XP spectra but is clearly present in the HREEL spectra. The HREELS deconvolution algorithm allows an otherwise obscured adsorbate spectrum to be observed. The spectra corroborate the presence of the surface

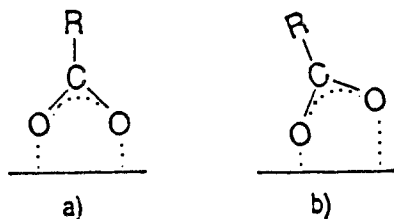
Table 3  
Carboxylate assignments. All frequencies are given in  $\text{cm}^{-1}$

	Formate	Acetate	Propionate
$\nu(\text{M}-\text{O})^a$	330		337
$\delta(\text{OCO})$	838	860	835
$\delta(\text{CH}_3)$	obs.	1302	1348
$\nu_s(\text{COO})$	1433	1502	1500
$\nu_a(\text{COO})$	1651	1650	1613
$\nu(\text{M}-\text{O}) + \nu_s(\text{COO})$	1763	obs.	1837
$\nu(\text{CH})$	3026	3075	3040
surface-OH	3533	3588	3593

<sup>a</sup>  $\nu(\text{M}-\text{O})$  by difference.

carboxylates and allow the symmetric carboxylate stretch to be observed, providing structural information not available from the XPS and undeconvoluted HREEL data alone.

It has previously been shown [8,31] that the frequency of the  $\nu_s(\text{COO})$  mode shifts to the relatively high value of  $\approx 1500 \text{ cm}^{-1}$  as the carboxylate binding changes from symmetric to a tilted bidentate form:



Because of the high symmetric stretch observed in the present studies, the adsorbate species proposed for the NiO(100) carboxylate system can be envisioned as adsorbing through the oxygen acid functionality to dissociate into a carboxylate and surface hydroxyl. Upon dissociation, the carbonyl oxygen attempts to bind to a nearest-neighbor nickel site but, perhaps because of the relatively long distance of 2.97 Å to this site, does not bind symmetrically and a “tilted” carboxylate results.

## 5. Conclusions

XPS and HREELS have been used to show that formic, acetic and propionic acids dissociate on NiO(100) at 300 K to give carboxylates and surface hydroxyls. Adsorption saturates after  $\approx 10000 \text{ L}$  to interact with two nickel surface sites in a tilted geometry. The HREELS results make use of an innovative deconvolu-

tion algorithm, allowing the adsorbate vibrational spectrum to be freed from the multiple excitation NiO(100) phonon spectrum.

## Acknowledgement

We gratefully acknowledge financial support from the American Chemical Society under PRF #18662-AC5 and NSF under #CHE-9117069.

## References

- [1] J. Lunsford, Chem. Ind. 22 (1985) 95.
- [2] H. Orita, S. Naito and K. Tamaru, J. Catal. 90 (1984) 183.
- [3] S.R. Bare, J.A. Stroschio and W. Ho, Surf. Sci. 155 (1985) L281.
- [4] N.R. Avery, Appl. Surf. Sci. 11/12 (1982) 774.
- [5] B.A. Sexton, A.E. Hughes and N.R. Avery, Surf. Sci. 155 (1985) 366.
- [6] P. Sen and C.N.R. Rao, Surf. Sci. 172 (1986) 269.
- [7] S.A. Isa, R.W. Joyner, M.H. Matloob and M.W. Roberts, Appl. Surf. Sci. 5 (1980) 345.
- [8] S.L. Miles, S.L. Bernasek and J.L. Gland, Surf. Sci. 127 (1983) 271.
- [9] P.T. Petrie and J.M. Vohs, Surf. Sci. 245 (1991) 315; 259 (1991) L750.
- [10] J.E. Crowell, J.G. Chen and J.T. Yates, J. Chem. Phys. 85 (1986) 3111.
- [11] J.B. Benziger, E.I. Ho and R.J. Maddix, J. Catal. 58 (1980) 149.
- [12] B.E. Hayden, H. Prince, D.P. Woodruff and A.M. Bradshaw, Surf. Sci. 133 (1983) 589.
- [13] X.D. Peng and M.A. Barteau, Surf. Sci. 224 (1989) 327.
- [14] J.M. Vohs and M.A. Barteau, Surf. Sci. 197 (1988) 109.
- [15] V.E. Henrich, Rep. Progr. Phys. 48 (1985) 1481.
- [16] M.A. Van Hove and P.M. Echenique, Surf. Sci. 82 (1979) L298.
- [17] M.R. Welton-Cook and M. Prutton, J. Phys. C13 (1980) 3993.
- [18] C.G. Kinniburgh and J.A. Walker, Surf. Sci. 63 (1977) 274.
- [19] M.A. Langell and R.P. Furstenau, Appl. Surf. Sci. 26 (1986) 445.
- [20] R.P. Furstenau and M.A. Langell, Surf. Sci. 159 (1985) 108.
- [21] J.M. McKay and V.E. Henrich, Phys. Rev. Lett. 53 (1984) 2343.
- [22] K.W. Wulser and M.A. Langell, J. Electron Spectry. Rel. Phenom., in press.
- [23] C.T. Au, W. Hirsch and W. Hirschwald, Surf. Sci. 199 (1988) 507.
- [24] P.A. Cox and A.A. Williams, Surf. Sci. 152/153 (1985) 791.
- [25] G. Dalmai-Imelik, J.C. Bertolini and J. Rousseau, Surf. Sci. 63 (1977) 67.
- [26] A.A. Lucas and M. Sunjic, Progr. Surf. Sci. 2 (1972) 75.
- [27] P.A. Cox, W.R. Flavell, A.A. Williams and R.G. Egdell, Surf. Sci. 152/153 (1985) 784.
- [28] D.D. Perrin, W.L.F. Armarego and D.R. Perrin, *Purification of Laboratory Chemicals* (Pergamon Press, Oxford, 1966).
- [29] N.H. Turner and A.M. Single, Surf. Interface Anal. 15 (1990) 215.
- [30] P.M.A. Sherwood, in: *Practical Surface Analysis by Auger and X-Ray Photoelectron Spectroscopy*, eds. D. Briggs and M.P. Seah (Wiley, New York, 1983) p. 445.
- [31] J.A.D. Matthew, M. Prutton, M.N. Gomati and D.C. Peacock, Surf. Interface Anal. 11 (1988) 173.
- [32] J.G. Chen, J.E. Crowell and J.T. Yates, Surf. Sci. 172 (1986) 733.